Hindawi
Journal of Chemistry
Volume 2020, Article ID 8428473, 11 pages
https://doi.org/10.1155/2020/8428473

Research Article

Using Modified Fly Ash for Removal of Heavy Metal Ions from Aqueous Solution

Thuy Chinh Nguyen,[1,2] **Trang Do Mai Tran**,[2] **Van Bay Dao**,[3] **Quoc-Trung Vu**,[3] **Trinh Duy Nguyen**,[4] **and Hoang Thai**[1,2]

[1]*Graduate University of Science and Technology, Vietnam Academy of Science and Technology, 18 Hoang Quoc Viet, Cau Giay, Hanoi 100000, Vietnam*
[2]*Institute for Tropical Technology, Vietnam Academy of Science and Technology, 18 Hoang Quoc Viet, Cau Giay, Hanoi 100000, Vietnam*
[3]*Faculty of Chemistry, Hanoi National University of Education, 136, Xuan Thuy, Cau Giay, Hanoi 100000, Vietnam*
[4]*NTT Institute of High Technology, Nguyen Tat Thanh University, 300A Nguyen Tat Thanh, District 4, Ho Chi Minh City 700000, Vietnam*

Correspondence should be addressed to Thuy Chinh Nguyen; thuychinhhn@gmail.com

Received 10 October 2019; Revised 5 February 2020; Accepted 28 February 2020; Published 23 March 2020

Academic Editor: Marcelino Maneiro

This paper presents the characteristics of fly ash which was modified by 2-mercaptobenzothiazole (MBT) and sodium dodecyl sulfate (SDS) as the surfactants after treating with 1M NaOH solution. The change in morphology, specific surface area, crystal structure, and composition of the unmodified and modified fly ash was evaluated by FTIR, XRD, FESEM, BET, and EDX methods and techniques. The FTIR spectra of modified fly ash showed that there was no chemical reaction between the surfactants and fly ash. The XRD patterns and FESEM images indicated that modified fly ash had zeolite structure with a pore size of about 50 nm. Heavy metal ion adsorption behavior as well as adsorption isotherm models (Langmuir and Freundlich) of Cd^{2+} and Hg^{2+} ions of the unmodified and modified fly ash were also investigated and discussed. The amount of adsorbed ions of the modified fly ash was higher than that of the unmodified fly ash. The calculated results from the adsorption data according to the adsorption isotherm models of the above ions displayed that the Langmuir isotherm model was complied for the Cd^{2+} adsorption process while the Freundlich isotherm model was fitted for the Hg^{2+} adsorption process.

1. Introduction

Application of fly ash (FA, waste product of thermal power plants) as additive/filler or adsorption material is opened and focused on study day to day. The main composition of FA includes inorganic oxides such as SiO_2, Al_2O_3, and Fe_2O_3 and a small fraction of Na_2O, MgO, and K_2O. High thermal stability and spherical shape are the advantages of FA to broaden its application [1].

One of the popular applications of FA is that it is used as a cheap absorbent for adsorption of heavy metal ions, organic substances, anions, dyes in water, and SOx, NOx, and mercury in air [2]. Chemical treatment of FA is an important tool to make FA a more effective absorbent for gas and water cleaning. In some reports, the authors studied on FA as zeolite for removal of heavy metal ions in solution [3–6] and catalytic [7], hydrocarbon contamination [8], lignite mine [9], oxamyl [10], resorcinol [11], phenol [12], and dye in waste water [13]. Based on an optical Fenton system, Visa et al. used FA to adsorb Cd^{2+} ion, methyl orange, and polyion water [14, 15]. Wang and Wu indicated that unburned carbon content in FA could influence on its adsorption ability [16]. FA is suggested as a promising absorbent for removal of various pollutants [17].

In 2002, Sarbak and Kramer-Wachowiak carried out experiments to treat FA by NaOH, $NaOH/NH_4HCO_3$, ethylenediamine tetraacetic acid (EDTA), and HCl solutions to change specific surface area and surface and porous

structure of FA. As a result, in all cases, the specific surface area and pore volume of treated FA were greater than those of original FA. The SEM images showed that the FA treated by HCl solution had surface smoother than the FA treated by $NaOH/NH_4HCO_3$ solution. The porosity of the treated FA was 10 times higher than that of the untreated FA. The treated FA is suitable for application as an adsorption material [1].

Agarwal et al. used NaOH-treated FA particles modified by cethyltrimethyl ammonium bromide (CTAB) (FA/NaOH/CTAB) for adsorption of resorcinol in waste water from plastic, dye, and cosmetic factories [11]. The authors showed that the size of FA/NaOH/CTAB was smaller than that of original FA as well as NaOH-treated FA. The specific surface area (calculated according to the BET method), pore volume, and diameter of the FA/NaOH/CTAB reached 51.12 m^2/g, 0.176996 cm^3/g, and 138.4928 Å, respectively. The resorcinol single layer adsorption efficiency of the FA/NaOH/CTAB was 500 mg/g in the range of pH 5–7 solutions. According to the authors, the resorcinol adsorption mechanism by FA/NaOH/CTAB at pH < 7 solutions was a combination of electrostatic attraction, hydrogen bonding, and organic partitioning. FA-based geopolymer was also used for removal of Li^+, Cs^+, Co^{2+}, Cs^{2+}, Sr^{2+}, and $AsO_4{}^3$ from solution [18, 19].

From literature findings, it can be inferred that FA particles has been treated by different agents such as acids or alkalis, EDTA, CTAB, or poly(1, 8-diaminonaphthalene) (PDAN). The treated FA particles have been used for adsorbing organic substances, Cr4+, Ni2+, and $Fe3^+$ ions. In our previous research studies, we investigated modification of FA by vinyltriethoxysilane [20], NaOH and H_2SO_4 solutions [21]. The treated FA was used for adsorption of Cd^{2+} and Hg^{2+} ions. The obtained results confirmed that the FA which was treated by the NaOH solution had a higher adsorption capacity than that by the acidic solution. The NaOH-treated FA modified by organic substances could improve the ions adsorption capacity of FA, leading to the potential application of FA as excellent adsorption materials. In some studies, the authors indicated that organic substances grafted onto the surface of FA could react with metal ions to form the complex [3–5]. As a result, percent removal of heavy metal ion using modified FA was increased significantly. Up to now, FA modified by 2-mercaptobenzothiazole (MBT) or sodium dodecyl sulfate (SDS) and use of the modified FA for Cd^{2+} and Hg^{2+} ions adsorption has not been studied. MBT has high affinity for Hg^{2+} ion; thus, MBT can contribute to the improvement of Hg^{2+} ion adsorption capacity for FA. SDS is a widely used surfactant which enhances dispersion of FA in water; therefore, it increases contact between Hg^{2+} ion and FA in aqueous solution. Therefore, in this work, NaOH-treated FA was modified by SDS and MBT, and the modified FA was used for removal of Cd^{2+} and Hg^{2+} from aqueous solution. The change in structure, morphology, composition as well as Cd^{2+} and Hg^{2+} adsorption capacity of modified FA was presented and discussed. The laboratory investigation results of Cd^{2+} and Hg^{2+} ions adsorption uptake from aqueous can be a reliable basic for applying the modified FA in treatment of waste water.

2. Experimental

2.1. Materials. Fly ash particles (FA) used in this work were provided by Pha Lai Thermal Power Plant (Vietnam). Total content of $SiO_2 + Fe_2O_3 + Al_2O_3$ in FA composition is higher than 86 wt.% (F class FA). Its particle size is in the range of 100–10 μm, and its humidity is 0.3%. 2-Mercaptobenzothiazole (MBT), sodium dodecyl sulfate (SDS), $HgCl_2$, and $CdCl_2$ were purchased from Merck Co. Some chemicals such as acetone and ethanol, which were obtained from China, were used without further purification.

2.2. Surface Modification of the Fly Ash. FA was treated by 1M NaOH solution (abbreviated as FAN) before being modified by SDS and MBT according to the process reported in [21]. The steps for modifying FAN by SDS and MBT were listed as follows. First, the FAN was added into the solution of 5% SDS (w/v) in water (the suitable content of SDS was chosen based on the data of experimental adsorption). The mixture (solid–liquid system) was stirred for 3 hours at 70°C with a stirring speed of 750 rpm. The mixture was continuously ultrasonic-stirred for 15 minutes before cooling in the air. Then, the SDS-modified FAN was washed by distilled water to remove residual surfactant. Finally, the solid was dried in a vacuum machine at 80°C until a constant weight is achieved, and SDS-modified FAN particles (abbreviated as FASDS) were obtained. The FASDS was reweighted and stored in a sealed PE bag.

To modify the FAN by MBT, 8% MBT (w/v) was dissolved in acetone solvent before adding FAN into the MBT-acetone solution (the suitable content of MBT was chosen based on the data of experimental adsorption). The mixture was stirred for 1 hour with a stirring speed of 750 rpm at room temperature. Then, the mixture was allowed for evaporating the solvent at room temperature. After that, filtering and washing the solid by ethanol and distilled water was performed before drying it in a vacuum machine at 80°C until a constant weight is achieved and MBT-modified FAN particles (abbreviated as FAMBT) were obtained. The FAMBT was reweighted and stored in a sealed PE bag.

2.3. Characterization

2.3.1. Infrared Spectroscopy (IR). IR spectra of the FAN and modified FAN particles were recorded by using a Nicolet iS10 spectrometer (USA) at room temperature from 400 to 4000 cm^{-1} by an average of 8 scans with a resolution of 8 cm^{-11}.

2.3.2. Field Emission Scanning Electron Microscopy (FESEM). FESEM images of the FAN and modified FAN particles were obtained using an S-4800 FESEM machine (Hitachi, Japan) to observe the change in morphology of the FAN and modified FAN particles.

2.3.3. X-Ray Diffraction (XRD). XRD analyses of the FAN and modified FAN particles were performed on a Siemens D5000 X-ray diffractometer (XRD) (CuK_α radiation source,

$\lambda = 0.154$ nm) at a generator voltage of 40 kV with a step of 0.03° and a current of 30 mA at a scan speed of 0.043°/s in the 2θ scan range from 5° to 90°.

2.3.4. Brunauer–Emmett–Teller (BET) Isotherm Equation. The specific surface area of the FAN and modified FAN particles was determined by the nitrogen sorption method (BET) on a Micromeritics Tristar 3000 device.

2.3.5. Energy-Dispersive X-Ray Spectroscopy (EDX). EDX spectra of the FAN and modified FAN particles were carried out on an EDX 6000E device (Japan).

2.3.6. Atomic Absorption Spectroscopy (AAS). This method was used to evaluate the adsorption effectiveness of the FAN and modified FAN particles on an AAS 3300 Perkin Elmer spectrophotometer (USA) and an AAS ICE 3500 spectrophotometer (USA).

2.4. Adsorption of Cd^{2+} and Hg^{2+} Ions by FA0, FAN, and Modified FAN Particles. 200 mg of FA samples was added into a 50 ml of solution containing Cd^{2+} or Hg^{2+} ion with different concentrations (ca. ppm). The mixture was stirred at room temperature for 120 minutes. This is the time for the heavy metal ion adsorption to reach the adsorption equilibrium. The pH value 6 was kept constant during the adsorption process. The amount of Cd^{2+} and Hg^{2+} ions adsorbed per gram of adsorbent, Q (mg·g^{-1}), was calculated using the following equation:

$$Q = \frac{(C_o - C_e)}{W}, \quad (1)$$

where Q is the amount of adsorbed metal ion at equilibrium conditions (metal ion (mg)/adsorbent (g)), V is the solution volume (L), and W is the sorbent mass (g). C_o and C_e are the initial and equilibrium concentrations of metal ions in solution (mg·L^{-1}), which are determined by the AAS method.

The removal of metal ions was calculated using the following equation:

$$H = \frac{(C_o - C_e) \cdot 100}{C_o}, \quad (2)$$

where H is the percent removal of metal ions (%).

All experiments were performed in triplicate.

2.5. Study on Adsorption Isotherms. In this work, the Langmuir and Freundlich isotherms have been selected for the study on ions adsorption behavior in solid–liquid system.

The Langmuir isotherm equation for ion adsorption can be written as follows:

$$q_e = \frac{q_{max} k_L C_e}{1 + k_L C_e}, \quad (3)$$

where C_e is the concentration of the solute at equilibrium (mol·L^{-1}) and q_e is the amount of the adsorbate adsorbed per unit weight of the adsorbent at equilibrium (mol·g^{-1}). The parameters, q_{max} and kL, are the Langmuir constants. q_{max} is represented as the maximum adsorption capacity, and k_L is related to the binding energy or affinity parameter of the adsorption system.The Freundlich isotherm is expressed as follows:

$$q_e = k_F C_e^{1/n_F}, \quad (4)$$

where k_F is the constant of the Freundlich isotherm (L$^{1/n}$ mg$^{(1-(1/n))}$g^{-1}) and $1/n_F$ is the Freundlich exponent.

3. Results and Discussion

3.1. Infrared Spectra of the FA0, FAN and Modified FAN Particles. IR spectra of the untreated FA (FA0), FAN, and modified FAN particles in Figure 1 show that the IR spectra of the FAN, FASDS, and FAMBT particles exhibit similar characteristic peaks. For example, the peaks at 3250–3700 cm^{-1} and 1640 cm^{-1} are for stretching and bending vibrations of hydroxyl group in the FA particles. The asymmetric, symmetric stretching, and bending vibrations of Si-O group in the FA particles correspond at 1070 cm^{-1}, 793 cm^{-1}, and 460 cm^{-1}, respectively [1, 22]. The peak at 555 cm^{-11} can be attributed for Al-O group in the FA particles. Interestingly, some new peaks in the IR spectrum of the FAMBT particles appeared at 2917 cm^{-1}, 2857 cm$^{-1,}$ and 1465 cm^{-1} corresponding to asymmetric, symmetric stretching, and bending vibrations of CH group in the heterocyclic structure of MBT. In addition, the peak observed at 1550 cm^{-1} characterizes for tertiary amine group in MBT. These can confirm that MBT was grafted onto the surface of the FAN particles after modification process [15, 22]. This is explained by the physical interactions (hydrogen bonding or dipolar-dipolar interaction) formed between hydroxyl groups on the surface of the FAN particles and the polar groups or element with a valence electron pair (SH, S) in MBT molecules. As a result, the MBT molecules were kept on the surface of the modified FAN particles.

To observe clearly, the position of characteristic peaks in the IR spectra of the FAN and modified FAN particles are listed in Table 1. The IR spectrum of the FA0 is not shown here because it was presented in our previous literature [21], but the main peaks are given in Table 1. The slight shift of some absorption peaks (1–5 cm^{-1}) can be caused by the effect of the surfactants (MBT and SDS). However, there is no chemical reaction between the surfactants and the FAN particles in the treatment process.

3.2. Morphology of the FA0, FAN, and Modified FAN Particles. FESEM images of the FA0 and FAN particles before and after modification are demonstrated in Figures 2 and 3. It can be observed that FA particles have spherical shape with the particle diameter in the range of 100–10 μm; however, their main particle size is in the range of 3–5 μm. This is the general size of the FA after sieving. The untreated FA (FA0) particles have a smooth surface while the treated FA (FAN) and modified FAN (FASDS and FAMBT particles) have rouge surfaces [23]. In addition, the micropores also

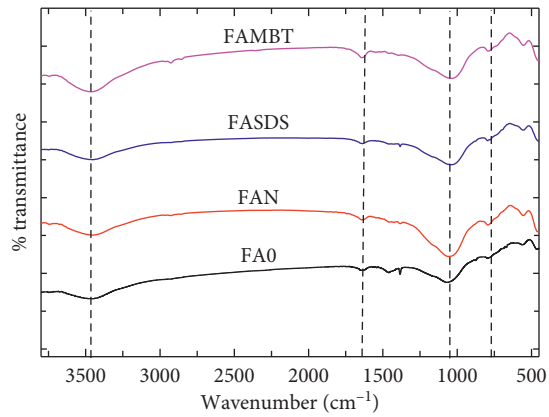

Figure 1: FTIR spectra of FA0, FAN, and modified FAN particles.

Table 1: Position of main peaks in FTIR spectra of FA0, FAN, and modified FAN particles.

Sample	Characteristic absorptions (cm^{-1})						
	$\delta_{\text{Si-O-Si}}$	$\delta_{\text{Al-O-Al}}$	$\nu_{\text{sym Si-O-Si}}$	$\nu_{\text{asym Si-O-Si}}$	δ_{OH}	ν_{SH}	ν_{OH}
FA0	461	557	793	1070	1636	—	3452
FAN	457	555	793	1057	1642	—	3451
FASDS	453	556	795	1036	1637	—	3452
FAMBT	454	553	790	1037	1642	2927, 2857	3455

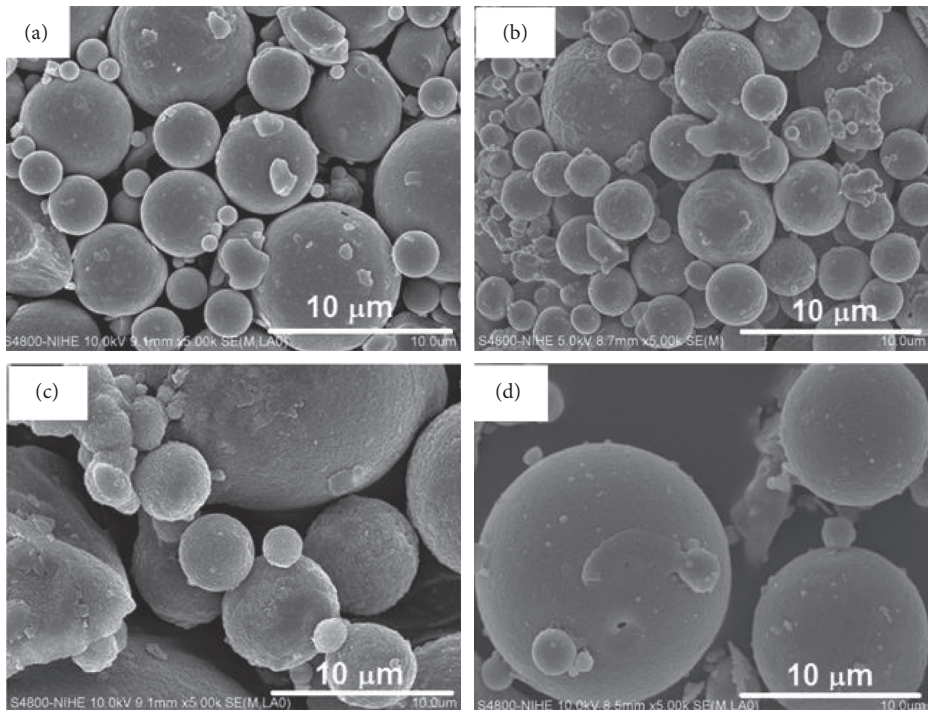

Figure 2: FESEM images of FA0 (a), FAN (b), FAMBT (c), and FASDS (d) particles at the magnification of 5.000 times.

appeared on the surface of the FAN, FASDS, and FAMBT particles, as shown higher magnification in Figure 3. These results prove that the surface of the FAN, FASDS, and FAMBT particles can be destroyed and cleaned by the effect of 1M NaOH solution and the surfactants. Besides, the occurrence of reaction between FA0 and NaOH ($2NaOH + Al_2O_3 \longrightarrow 2NaAlO_2 + H_2O$; $NaOH + Al_2O_3 + SiO_2 \longrightarrow Na_2O{\cdot}Al_2O_3{\cdot}nSiO_2{\cdot}mH_2O$) can lead to formation of micropores on the surface of the FAN, FASDS, and FAMBT particles due to the dissolution of aluminum oxide and silica oxide into the solution in the treatment process. In comparison to the FASDS and

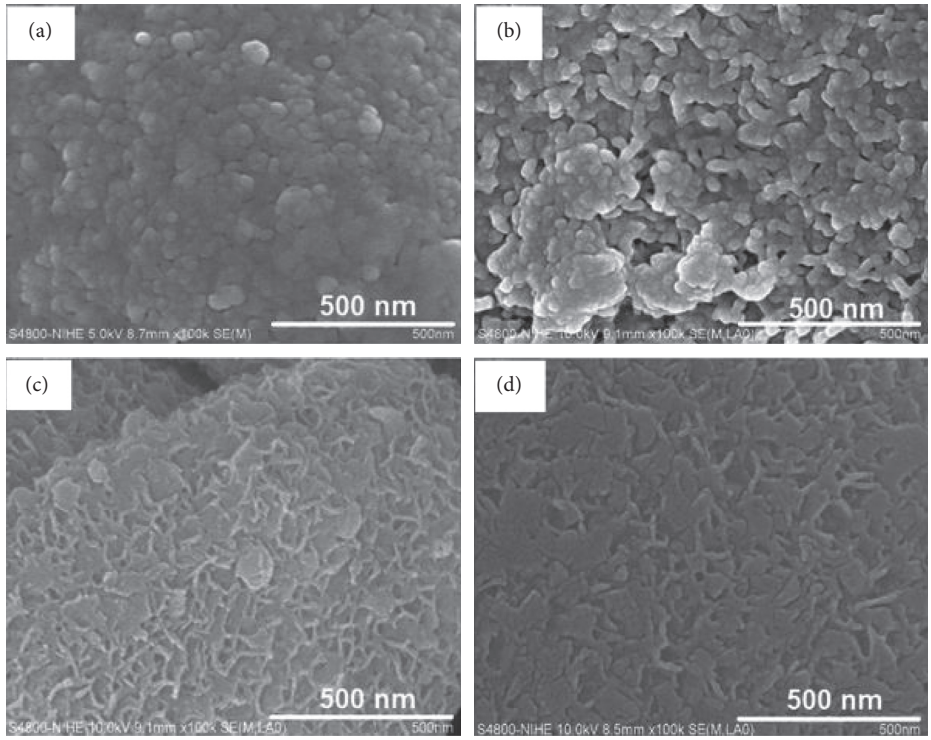

Figure 3: FESEM images of FA0 (a), FAN (b), FAMBT (c), and FASDS (d) particles at the magnification of 100.000 times.

FAMBT particles, it can be clearly seen that the surface of the FAMBT particles becomes rougher and jagged than those of the FASDS particles. The size and number of micropores (ca. 50 nm) of the FAMBT particles are smaller but higher than those of the FASDS particles. Paulina Halas also indicated that as for zeolite from fly ash, single crystals with irregular conformation and size 3–6 mm are demonstrated and the edges of the particles are often sharp and jagged [5].

3.3. Crystal Structure of the FAN and Modified FAN Particles. The change in crystal structure of the unmodified and modified FAN particles is evaluated according to the XRD patterns presented in Figure 4. As reported in our previous research [21] and some other research studies [3–5, 24], the XRD spectrum of the FA demonstrates that the structure of FA0 particles is composed of mullite, quartz, and hematite while the FAN particles has a zeolite P ($Na_6Al_6Si_{10}O_{32}.12H_2O$ or NaP) structure (at $2\theta = 13^\circ$, $2\theta = 16^\circ$, $2\theta = 27^\circ$, and $2\theta = 55^\circ$). The appearance of NaP phase could be caused by the effect of NaOH solution on the conversion of alumino-silicate materials by the reaction between NaOH solution with SiO_2 and Al_2O_3 in the FA particles as abovementioned in Section 3.2. Grigorios et al. also mentioned that the polarization of chemical bonds in FAN particles led to the improvement of their active centers in the frame of FAN particles. As a result, the terminal groups (≡Si–OH, ≡Si–ONa, ≡Si–O– and $(\equiv Si–O)_3Al–O–$) of FA particles are increased as treated by NaOH solution [8]. The crystal structure of FASDS and FAMBT particles is similar to that of FAN particles but the intensity of peaks which characterized for NaP zeolite phase in the XRD

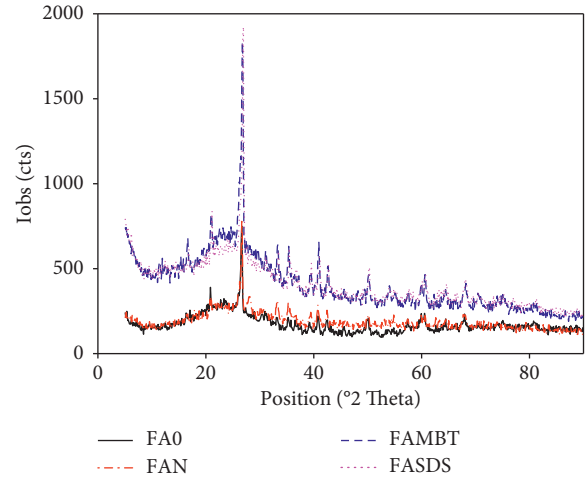

Figure 4: XRD patterns of FA0, FAN, and modified FAN particles.

pattern of the FASDS and FAMBT samples is three times higher than that of the FAN particles. This result proves that the NaP zeolite phase in the crystal structure of FASDS and FAMBT particles is stronger and clearer than that in FAN particles.

3.4. Change in Composition of the FA Samples after Modification. Figure 5 and Table 2 display EDX spectra and element weight percentage of the FA0, FAN, and modified FAN particles. Three positions were chosen to record the EDX spectrum for every sample, and the data shown in Table 2 are the average values. It can be observed that O, Al,

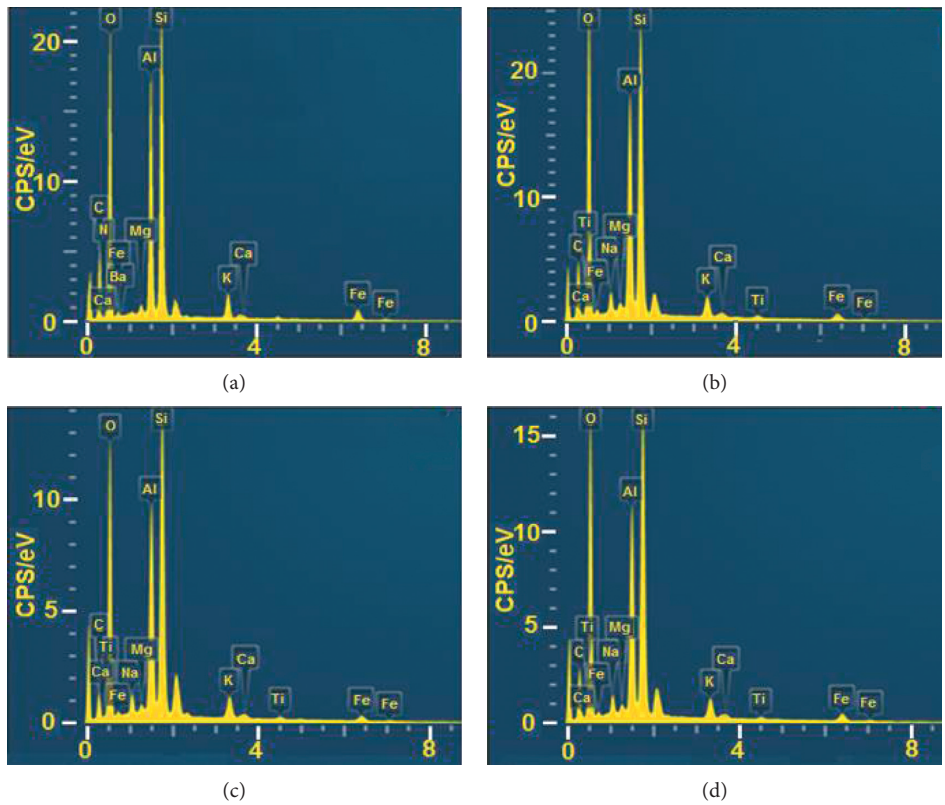

Figure 5: EDX spectra of FA0 (a), FAN (b), FAMBT (c), and FASDS (d).

Table 2: Weight percent of elements in FA0, FAN, and modified FAN particles.

Element	Sample			
	FA0	FAN	FASDS	FAMBT
C	28.10	26.49	26.94	17.89
O	44.35	48.40	47.61	49.62
Al	7.56	8.32	7.87	11.80
Si	10.65	11.42	12.07	14.93
Na	—	1.08	0.99	0.92
K	1.71	1.57	1.56	1.96
Fe	2.48	1.84	2.09	1.97
Mg	1.55	0.31	0.33	0.27
Ca	0.25	0.28	0.27	0.31
N	3.01	—	—	—
Ba	0.33	—	—	—
Ti	—	0.28	0.28	0.34
Total	100	100	100	100

Si, and Fe are the main elements in all investigated FA samples due to the main composition of the FA particles including main oxides such as SiO_2, Al_2O_3, and Fe_2O_3. The order of other elements is K, Mg, and Ca. The existence of C and N elements in the FA0 particles could be unburned carbon and organic impurities.

The presence of Na element in the FAN, FASDS, and FAMBT particles can be attributed for appearance of NaP zeolite phase as discussed in XRD (Section 3.3). The decrease in weight percentage of C element as well as the disappearance of Ba and N elements in the FAN, FASDS, and FAMBT particles is due to the removal of unburned carbon, organic impurities, and BaO from the FAN, FASDS, and FAMBT particles. The weight percentage of Fe, Ca, and K elements in the FAN particles changed insignificantly after modification by SDS and MBT. This shows that the oxides and subtances of Fe, Ca, and K in FASDS and FAMBT particles are relatively stable, unaffected by the NaOH solution or surfactants. Interestingly, the increase in weight percentages of Al and Si elements and the presence of Ti element after the modification process are the evidence for structural damage and surface erosion as displayed in FESEM images. The Ti element does not appear in the FA0 sample due to its deep location in the FA0 structure. On the other side, weight percentages of the Al and Si elements are rised by the formation of NaP zeolite phase. This result is similar to the above XRD result.

3.5. Change in Specific Surface Area of the FA0, FAN, and Modified FAN Particles. Figure 6 shows the performance of nitrogen adsorption and desorption of the FA0, FAN, and modified FAN particles. According to the IUPAC classification of adsorption isotherms, based on the adsorption and desorption pathways of samples, it can be seen that the adsorption and desorption isotherms are type IV with hysteresis. The type A of hysteresis loop on the adsorption-desorption isotherms corresponded to the cylindrical micropore structure of the FAN, FAMBT, and FASDS particles. Table 3 lists the specific surface area (SSA), pore volume, and

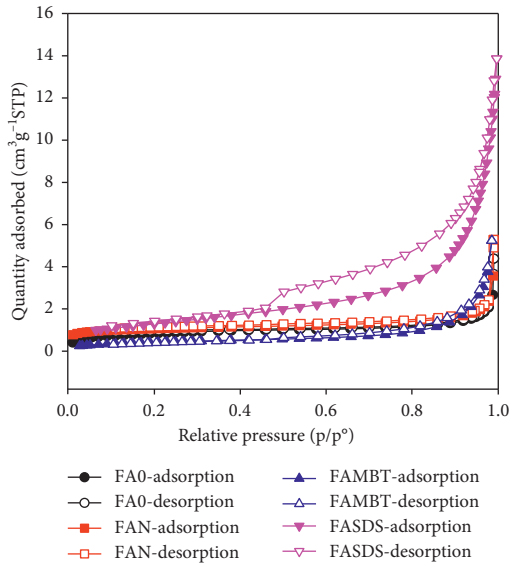

Figure 6: Nitrogen adsorption-desorption curves of FA0, FAN, and modified FAN particles.

pore diameter of the FA0, FAN, and modified FAN particles. The SSA of FAN and FASDS particles is increased while the SSA of the FAMBT particles is decreased in comparison with that of the FA0 particles. In the case of SDS grafted onto the FAN particles, it is difficult to form the physical interaction between SDS and the FAN particles because there is no element with a valence electron pair in SDS molecules; hence, SDS was not kept on the surface of FAN particles. The play of SDS as a detergent is stronger than that as a grafting agent. Therefore, the SSA and pore diameter of the FASDS particles are slightly increased in comparison with the FAN particles. When using MBT for the modification of the FAN particles, the organic layer on the surface of the FAN particles can cover the micropores leading to the reduction of SSA and increase in the pore diameter of the FAMBT particles in comparison with that of the FAN particles [11, 25].

Interestingly, the pore volume of the FASDS and FAMBT particles (0.0194 and 0.0056 $cm^3\,g^{-1}$) are also larger than those of the FA0 and FAN particles. This can be related to the some metal ion adsorption capacity of the FASDS and FAMBT particles as discussed below.

3.6. Cd^{2+} and Hg^{2+} Ion Adsorption Capacity of the FA0, FAN, and Modified FAN Particles

3.6.1. Choosing the Most Suitable Type of FA for Cd^{2+} Ion Adsorption. The percent removal of Cd^{2+} ion (H) and the amount of adsorbed Cd^{2+} ion at equilibrium conditions (Q) obtained from Cd^{2+} ion adsorption process by the FA0, FAN, and modified FAN particles at the same initial Cd^{2+} ion concentration and the same FA weight are determined from data obtained by AAS analysis and are given in Table 4.

Here, a and b are the parameters obtained from the calibration equation of Cd^{2+} ion, f is the dilution coefficient, and Abs is the optical absorption of solution.

From data in Table 4, the FAMBT particles exhibit the highest H and Q values (97% and 12.14 $mg{\cdot}g^{-1}$, respectively) while the FA0 particles have the lowest H and Q values (65% and 8.23 $mg{\cdot}g^{-1}$, respectively). The increase in percent removal of Cd^{2+} ion using the FAMBT particles can be explained by the rising its pore diameter in comparison with that of the FAN and FASDS particles (as listed in Table 3) as well as the formation of complex between MBT and Cd^{2+} ion (Figure 7) [25]. Based on these results, the FAMBT particles can be the most suitable FA particles for further study on Hg^{2+} and Cd^{2+} adsorption.

3.6.2. Cd^{2+} Adsorption Behavior by FAMBT Particles. Figure 8 presents the influence of initial Cd^{2+} concentration on percent removal of Cd^{2+} ion (H) and the amount of adsorbed Cd^{2+} ion at equilibrium conditions (Q) of the FAMBT particles. It is clear that the decrease in percent removal of Cd^{2+} ion occurs as well as the increase in the amount of adsorbed Cd^{2+} ion of the FAMBT particles. At Cd^{2+} concentration lower than 30 $mg\,L^{-1}$ (or 30 ppm), the percent removal of Cd^{2+} ion by the FAMBT particles is quite high, from 98.95 to 99.47%. Therefore, the FAMBT particles are appropriate for Cd^{2+} adsorption at a concentration lower than 30 ppm in treatment of factory or domestic waste water. The high percent removal of Cd^{2+} ion of FAMBT particles could be explained by formation of the complex between Cd^{2+} and MBT grafted onto the surface of the FAN particles as shown in Figure 7. On the other side, high percent removal of Cd^{2+} ion of FAMBT particles was also caused by the uniform adsorption layer of Cd^{2+} ion at adsorption centers. In order to study on the Cd^{2+} adsorption mechanism of FAMBT particles clearly, the Freundlich and Langmuir isotherms are used for investigation of Cd^{2+} adsorption behavior by FAMBT particles [10, 12].

Langmuir and Freundlich isotherms of Cd^{2+} adsorption by the FAMBT particles are expressed in Figure 9. The Langmuir and Freundlich isotherm parameters are also presented in Table 5. Owing to Figure 9 and data in Table 5, the regression coefficients (R^2) obtained from the Langmuir isotherm model is greater than that from the Freundlich isotherm model. Therefore, the Langmuir isotherm model is more suitable for reflecting the Cd^{2+} adsorption behavior of FAMBT particles. The maximum monolayer adsorption capacity (Q_{max}) of the FAMBT particles is 12.4 mg/g. The Cd^{2+} adsorption is a single layer adsorption and active centers on the surface of the FAMBT particles have same adsorption energy. Cd^{2+} ions adsorbed on the surface of the FAMBT particles do not interact with each other. The existence of a maximum absorbance capacity of FAMBT particles can show the formation of a saturation single layer of heavy metal ions on the surface of FAN particles.

3.6.3. Hg^{2+} Adsorption Behavior by FAMBT Particles. The Hg^{2+} adsorption behavior of the FAMBT particles is similar to the Cd^{2+} adsorption behavior with the decrease in the percent removal of Hg^{2+} ion and increase in the amount of adsorbed Hg^{2+} ion (Figure 10). However, the percent removal of Hg^{2+} ion of the FAMBT particles is lower than

Table 3: Specific surface area, pore volume, and pore diameter of FA0, FAN, and modified FAN particles.

Sample	Specific surface area (m^2/g)	Pore volume (cm^3/g)	Pore diameter (nm)
FA0	2.9489	0.0031	11.3126
FAN	3.5178	0.0043	15.2018
FASDS	4.7190	0.0194	16.4493
FAMBT	1.5275	0.0056	20.0612

Table 4: Cd^{2+} adsorption parameters by FA0, FAN, and modified FAN particles.

Sample	a	b	f	Abs	kq mg/l	H (%)	Q (mg/g)
FAMBT	0.2691	0.0043	5	0.082	1.44	97	12.14
FASDS	0.2691	0.0043	5	0.318	5.83	88	11.04
FAN	0.2691	0.0043	25	0.088	7.78	84	10.55
FA0	0.2691	0.0043	25	0.188	17.07	65	8.23

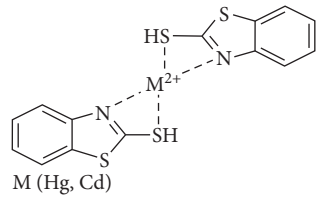

Figure 7: General formula of M-MBT complex (M = Hg, Cd).

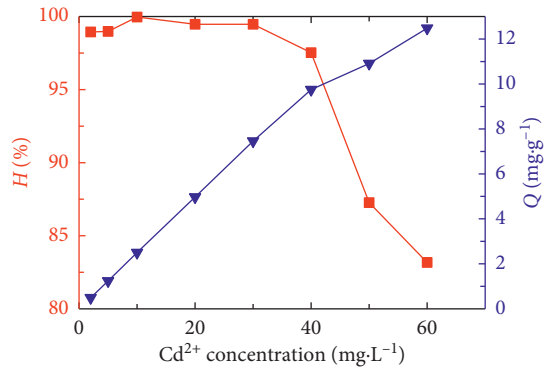

Figure 8: Percent removal of Cd^{2+} ion H (-■-) and the amount of adsorbed Cd^{2+} ion at equilibrium conditions Q (-▲-) of the FAMBT particles at different Cd^{2+} concentrations.

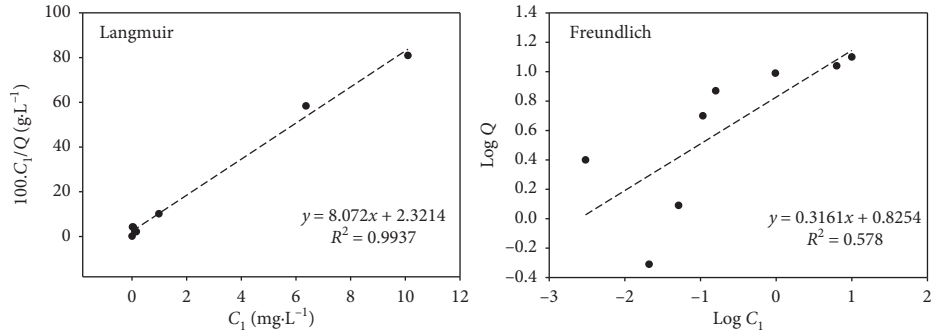

Figure 9: Langmuir and Freundlich adsorption isotherms reflecting Cd^{2+} adsorption by the FAMBT particles.

Table 5: Langmuir and Freundlich isotherm parameters reflecting Cd^{2+} adsorption by the FAMBT particles.

Langmuir		Freundlich	
Parameter	Value	Parameter	Value
Q_{max} (mg/g)	12.40	n_F	3.16
k_L	3.50	k_F	$10^{3.16}$
R^2	0.99	R^2	0.58

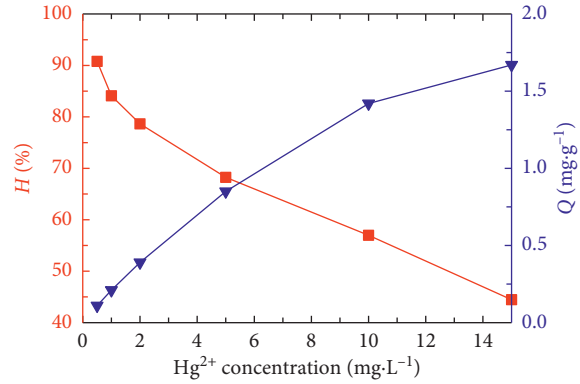

Figure 10: Influence of percent removal of Hg^{2+} ion H (-■-) and amount of adsorbed Hg^{2+} ion at equilibrium conditions Q (-▲-) on initial Hg^{2+} concentration (adsorbent of FAMBT).

Table 6: Langmuir and Freundlich isotherm parameters reflecting Hg^{2+} ion adsorption by the FAMBT particles.

Langmuir		Freundlich	
Parameter	Value	Parameter	Value
Q_{max} (mg/g)	1.91	n	1.85
k_L	0.72	k_F	$10^{1.85}$
R^2	0.98	R^2	0.99

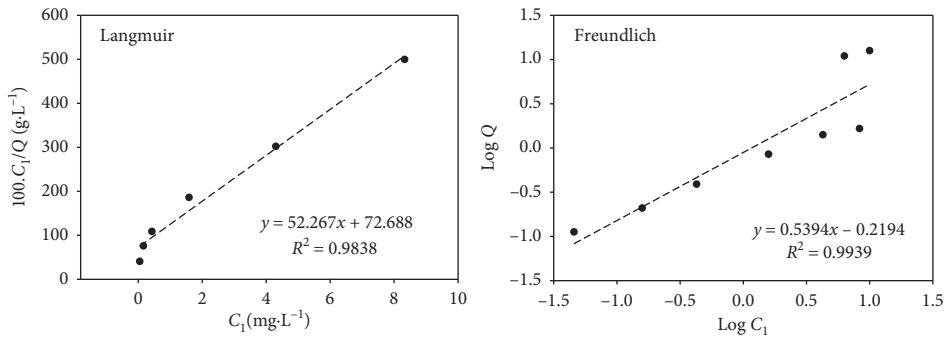

Figure 11: Langmuir and Freundlich adsorption isotherms reflecting Hg^{2+} ion adsorption by the FAMBT particles.

Table 7: Comparison of maximum adsorption capacity (Q_{max}) of different adsorbents for Hg^{2+} and Cd^{2+} ions.

Adsorbent	Maximum adsorption capacity—Q_{max} (mg·g^{-1})		Ref.
	Hg^{2+} ions	Cd^{2+} ions	
Activated carbon from *Xanthoceras sorbifolia* Bunge hull	235.6	388.7	[26]
Clay mineral montmorillonite	0.86	—	[27]
Graphenes magnetic material	23.03	27.83	[28]
Chitosan	52.63	58.8	[29]
FAMBT	1.91	12.4	This work

that of the percent removal of Cd^{2+} ion. It reaches to 90.80% and 84.10% corresponding to Hg^{2+} concentration of 0.5 and 1 ppm, respectively, and it falls down fast at Hg^{2+} concentration in the range of 2–15 ppm. This phenomenon can be explained similarly in the report of Xiaotao et al. Cd^{2+} ions about higher affinity for FA-modified MBT, which may be attributed to the fact that a longer ionic radius (Cd^{2+}(97 pm) < Hg^{2+}(110 pm)) corresponds to a shorter hydrated ionic radius, resulting in the higher affinity for metal ions of FA-modified MBT [26].

Based on the data of Hg^{2+} adsorption, it can be suggested that the FAMBT particles is suitable for Hg^{2+} adsorption at a concentration lower than 1 ppm when application of the FAMBT particles in treatment to factory, urban, and domestic waste water.

From the data listed in Table 6 and (Figure 11), the Freundlich isotherm model is more appropriate than the Langmuir isotherm model for reflecting the Hg^{2+} adsorption behavior by the FAMBT particles due to higher regression coefficients ($R^2 = 0.99$). We also compared the capacity of proposed adsorbent in the removal of Hg^{2+} and Cd^{2+} ions from aqueous with the results published by other authors as shown in Table 7. From the data in Table 7, it can be seen that the selectivity of modified FA and some other absorbents toward metal ions is found to be in the order Cd^{2+} ions > Hg^{2+} ions. This selectivity sequence may be caused by the basis of the first hydrolysis constant values for Hg^{2+} and Cd^{2+} ions. The hydrolyzed metal ions are more strongly sorbed than free metal ions. Since Cd^{2+} ions have smaller hydrated ionic radii than Hg^{2+} ions corresponding to fewer weakly bonded water molecules, Cd^{2+} ions tend to move faster to the potential adsorption sites on absorbents. On the other hand, the higher electronegativity of Cd^{2+} ions can also lead to a greater reaction with potential adsorption sites in absorbents as compared to Hg^{2+} ions [30].

4. Conclusions

In conclusion, the structure, morphology, and some other characteristics of FAN particles have been changed significantly after modification by MBT and SDS surfactants. The surface of the FASDS and FAMBT samples is rougher than that of the FA0 and FAN particles. The specific surface area of the samples is arranged in the order FASDS > FAN > FAMBT > FA0. The NaP phase in the structure of the FAMBT and FASDS particles appears clearer and stronger than that of the FAN particles. The FAMBT sample is chosen for study on Cd^{2+} and Hg^{2+}adsorption because of its highest percent removal of ions among four tested samples. The Cd^{2+} and Hg^{2+}adsorption behavior of the FAMBT sample is similar with a decrease in the percent removal of ions as increasing the heavy metal ion concentration. The Langmuir isotherm model is complied with Cd^{2+} adsorption ($R^2 = 0.99$) while the Freundlich is suitable for study on Hg^{2+}adsorption ($R^2 = 0.99$). The modified FA is a promising absorbent for removal of Hg^{2+} and Cd^{2+} ions in waste water.

Data Availability

The data used to support the findings of this study are included within the article.

Conflicts of Interest

There are no conflicts of interest to declare.

Acknowledgments

This work has been financially supported by the Vietnam Academy of Science and Technology for Young Scientists.

References

[1] Z. Sarbak and M. Kramer-Wachowiak, "Porous structure of waste fly ashes and their chemical modifications," *Powder Technology*, vol. 123, no. 1, pp. 53–58, 2002.

[2] V. P. Suhas, C. N. Suryakant, and J. K. Sunil, "Industrial applications of fly ash: a Review," *International Journal of Science, Engineering and Technology Research*, vol. 2, no. 9, pp. 1659–1663, 2013.

[3] S. Mengting, L. Guangqian, Z. Hailu et al., "Surface modification of fly ash by non-thermal air plasma for elemental mercury removal from coal-fired flue gas," *Environmental Technology*, pp. 1–12, 2019.

[4] X. D. Ji, Y. Y. Ma, S. H. Peng, Y. Y. Gong, and F. Zhang, "Simultaneous removal of aqueous Zn^{2+}, Cu^{2+}, Cd^{2+}, and Pb^{2+} by zeolites synthesized from low-calcium and high-calcium fly ash," *Water Science & Technology*, vol. 76, no. 7-8, pp. 2106–2119, 2017.

[5] P. Halas, D. Kolodynska, A. Plaza, M. Geca, and Z. Hubicki, "Modified fly ash and zeolites as an effective adsorbent for metal ions from aqueous solution," *Adsorption Science & Technology*, vol. 35, no. 5-6, pp. 519–533, 2017.

[6] E. Pehlivan and S. Cetin, "Application of fly ash and activated carbon in the removal of $Cu^{2+}$and Ni^{2+} ions from aqueous solutions," *Energy Sources, Part A: Recovery, Utilization, and Environmental Effects*, vol. 30, no. 13, pp. 1153–1165, 2008.

[7] S. Vichaphund, D. Aht-Ong, V. Sricharoenchaikul, and D. Atong, "Characteristic of fly ash derived-zeolite and its catalytic performance for fast pyrolysis of Jatropha waste," *Environmental Technology*, vol. 35, no. 17, pp. 2254–2261, 2014.

[8] J. Sasithorn, D. Wiwattanadate, and S. Sangsuk, "Utilization of fly ash from power plant for adsorption of hydrocarbon contamination in water," *Journal of Metals, Materials and Minerals*, vol. 20, no. 1, pp. 5–10, 2010.

[9] I. Grigorios, K. Athanasios, K. Nikolaos, and V. Charalampos, "Zeolite development from fly ash and utilization in lignite mine-water treatment," *International Journal of Mineral Processing*, vol. 139, pp. 43–50, 2000.

[10] D. Singh, "Studies of the adsorption thermodynamics of oxamyl on fly ash," *Adsorption Science & Technology*, vol. 18, no. 8, pp. 741–748, 2000.

[11] S. Agarwal and A. Rani, "Adsorption of resorcinol from aqueous solution onto CTAB/NaOH/flyash composites: equilibrium, kinetics and thermodynamics," *Journal of Environmental Chemical Engineering*, vol. 5, no. 1, pp. 526–538, 2017.

[12] R. Sharan, G. Singh, and S. K. Gupta, "Adsorption of phenol from aqueous solution onto fly ash from a thermal power

plant," *Adsorption Science & Technology*, vol. 27, no. 3, pp. 267–279, 2009.

[13] D. Chatterjee, V. R. Patnam, A. Sikdar, and S. K. Moulik, "Removal of some common textile dyes from aqueous solution using fly ash," *Journal of Chemical & Engineering Data*, vol. 55, no. 12, pp. 5653–5657, 2010.

[14] M. Visa and A. Duta, "Methyl-orange and cadmium simultaneous removal using fly ash and photo-Fenton systems," *Journal of Hazardous Materials*, vol. 244-245, pp. 773–779, 2013.

[15] M. Visa, L. Isac, and A. Duta, "Fly ash adsorbents for multication wastewater treatment," *Applied Surface Science*, vol. 258, no. 17, pp. 6345–6352, 2012.

[16] S. Wang and H. Wu, "Environmental-benign utilisation of fly ash as low-cost adsorbents," *Journal of Hazardous Materials*, vol. 136, no. 3, pp. 482–501, 2006.

[17] C. G. Jun, K. Y. Sam, and J. C. Nag, "Application of fly ash as an adsorbent for removal of air and water pollutants," *Applied Sciences*, vol. 8, no. 7, p. 1116, 2018.

[18] T. Quanzhi and S. Keiko, "Application of fly ash-based geopolymer for removal of cesium, strontium and arsenate from aqueous solutions: kinetic, equilibrium and mechanism analysis," *Water Science & Technology*, vol. 79, no. 11, pp. 2116–2125, 2019.

[19] T. Quanzhi and S. Keiko, "Structural characterizations of fly ash-based geopolymer after adsorption of various metal ions," *Environmental Technology*, pp. 1–11, 2019.

[20] V. M. Trong, V. M. Tuan, N. T. Chinh et al., "Characterization of fly ash modified with vinyltriethoxysilane," *Journal of Nanoscience and Nanotechnology*, vol. 15, no. 8, pp. 5905–5909, 2015.

[21] N. T. Chinh, T. T. Mai, N. T. T. Trang, N. T. T. Huong, and T. Hoang, "Using fly ash treated by NaOH and H_2SO_4 solutions for Hg^{2+} and Cd^{2+} ion adsorption," *Vietnam Journal of Chemistry*, vol. 55, no. 2, pp. 196–201, 2017.

[22] J. Xie, S. Wu, L. Pang, J. Lin, and Z. Zhu, "Influence of surface treated fly ash with coupling agent on asphalt mixture moisture damage," *Construction and Building Materials*, vol. 30, pp. 340–346, 2012.

[23] P. Bably, M. Sudip, S. Kumari, K. M. Arun, and J. G. M. Robert, "Studies on synthesis and characteristics of zeolite prepared from Indian fly ash," *Environmental Technology*, vol. 33, no. 1, pp. 37–50, 2012.

[24] Y. R. Wang, D. C. W. Tsang, W. E. Olds, and P. A. Weber, "Utilizing acid mine drainage sludge and coal fly ash for phosphate removal from dairy wastewater," *Environmental Technology*, vol. 34, no. 24, pp. 3177–3182, 2013.

[25] Y. Qing, L. Nan, C. Yue et al., "Effect of large pore size of multifunctional mesoporous microsphere on removal of heavy metal ions," *Journal of Hazardous Materials*, vol. 254–255, pp. 157–165, 2013.

[26] Z. Xiaotao, H. Yinan, W. Ximing, C. Zhangjing, and L. Chun, "Competitive adsorption of cadmium(II) and mercury(II) ions from aqueous solutions by activated carbon from *Xanthoceras sorbifolia* Bunge hull," *Journal of Chemistry*, vol. 2016, Article ID 4326351, 10 pages, 2016.

[27] C. Green-Ruiz, "Adsorption of mercury(II) from aqueous solutions by the clay mineral montmorillonite," *Bulletin of Environmental Contamination and Toxicology*, vol. 75, no. 6, pp. 1137–1142, 2005.

[28] X. Guo, B. Du, Q. Wei et al., "Synthesis of amino functionalized magnetic graphenes composite material and its application to remove Cr(VI), Pb(II), Hg(II), Cd(II) and Ni(II) from contaminated water," *Journal of Hazardous Materials*, vol. 278, pp. 211–220, 2014.

[29] S. Soheil, Z. Raziyeh, A. Javanshir-Khoei, H. Seyed Mehdi, M. Mehran, and D. Parisa, "Removal of Hg (II) and Cd (II) ions from aqueous solution using chitosan: kinetics and equilibrium studies," *Iranian Journal of Health Sciences*, vol. 3, no. 2, pp. 21–30, 2015.

[30] E. Sočo and J. Kalembkiewicz, "Comparison of adsorption of Cd(II) and Pb(II) ions on pure and chemically modified fly ashes," *Chemical and Process Engineering*, vol. 37, no. 2, pp. 215–234, 2016.